

An SSFP Signal Equation with Finite RF Pulses and Exchanging Water Pools

Tobias C Wood¹, Samuel A Hurley², Gareth J Barker¹, and Steven C R Williams¹

¹Neuroimaging, King's College London, Institute of Psychiatry, London, London, United Kingdom, ²Medical Physics, University of Wisconsin, Wisconsin, United States

Introduction: Previous derivations of the signal equation for Steady-State Free Precession (SSFP) sequences mostly treat the excitation RF pulse as happening instantaneously. For sequences such as balanced-SSFP (bSSFP) this assumption may not be accurate as the RF pulse length may be around 20% of the total repetition time. Recently Bieri et al [1] derived a bSSFP signal equation that accounted for RF pulse length by means of a correction factor that approximates the amount of time the net magnetization lies approximately along the longitudinal axis. However this equation cannot be applied to multi-component SSFP signal equations because the correction factor would be different for each component. We present here an alternate derivation of the SSFP signal at the echo time with finite-length RF pulses that can easily be extended to multiple water pools.

Theory: Previous to Bieri et al, Jaynes [2] derived a general expression for the signal from a cyclic sequence where RF pulses are modeled by solving the Bloch equation while including an infinitesimal rotation $\delta\alpha$ about the x-axis. We also include an infinitesimal rotation $\delta\omega$ about the z-axis to model off-resonance and a discrete rotation ϕ after each TR to describe phase-cycling. The matrix Φ can also be used to model spoiling in an SPGR sequence by setting all elements except the bottom-right to zero. \mathbf{m}_∞ and \mathbf{r}_∞ refer to the equilibrium magnetization with the RF pulse switched off and on respectively. We then find the steady-state magnetization \mathbf{r}_{ss} after, instead of before, the RF pulse and apply the Bloch equation once more to find the signal \mathbf{m}_e at the echo time. For multi-component systems this is an important step as the signal from each pool will decay with different T_2 .

$$\mathbf{R} = \begin{bmatrix} 1/T_2 & 0 & 0 \\ 0 & 1/T_2 & 0 \\ 0 & 0 & 1/T_1 \end{bmatrix} \quad \Phi = \begin{bmatrix} \cos \phi & \sin \phi & 0 \\ -\sin \phi & \cos \phi & 0 \\ 0 & 0 & 1 \end{bmatrix} \quad \Lambda_{\mathbf{R}}(t) = \exp(-(\mathbf{R} + \Omega + \mathbf{A})t)$$

$$\mathbf{A} = \begin{bmatrix} 0 & 0 & 0 \\ 0 & 0 & -\delta\alpha \\ 0 & \delta\alpha & 0 \end{bmatrix} \quad \Omega = \begin{bmatrix} 0 & -\delta\omega & 0 \\ \delta\omega & 0 & 0 \\ 0 & 0 & 0 \end{bmatrix} \quad \Lambda(t) = \exp(-(\mathbf{R} + \Omega)t)$$

$$\mathbf{r}_{ss} = (\mathbf{I} - \Lambda_{\mathbf{R}}\Phi\Lambda)^{-1} (\Lambda_{\mathbf{R}}\Phi(\mathbf{I} - \Lambda)\mathbf{m}_\infty + (\mathbf{I} - \Lambda_{\mathbf{R}})\mathbf{r}_\infty)$$

$$\mathbf{m}_e = \Lambda(T_E) \times (\mathbf{m}'_n - \mathbf{m}_\infty) + \mathbf{m}_\infty$$

Exchange between two magnetization components \mathbf{a} and \mathbf{b} is then included by combining the magnetizations into a joint magnetization vector \mathbf{m}_j and adding a matrix \mathbf{K}_j to the evolution matrices that includes the exchange constants between the components [3]. We order the joint magnetization vector in a different way to that used previously [3, 4] which simplifies the joint evolution matrices to diagonal block form, permitting the separation of exchanging and non-exchanging water pools to different equation systems. For a three component model [4] this improves computation speed by a factor of three compared to the original ordering. The above equations for \mathbf{r}_{ss} and \mathbf{m}_e can then be used without further modification.

$$\mathbf{m}_j - \begin{bmatrix} a_x \\ a_y \\ a_z \\ b_x \\ b_y \\ b_z \end{bmatrix} \quad \mathbf{K}_j - \begin{bmatrix} k_{ab} & 0 & 0 & -k_{ba} & 0 & 0 \\ 0 & k_{ab} & 0 & 0 & -k_{ba} & 0 \\ 0 & 0 & k_{ab} & 0 & 0 & -k_{ba} \\ -k_{ab} & 0 & 0 & k_{ba} & 0 & 0 \\ 0 & -k_{ab} & 0 & 0 & k_{ba} & 0 \\ 0 & 0 & -k_{ab} & 0 & 0 & k_{ba} \end{bmatrix} \quad \mathbf{R}_j = \begin{bmatrix} \mathbf{R}_a & 0 \\ 0 & \mathbf{R}_b \end{bmatrix} \quad \mathbf{A}_j = \begin{bmatrix} \mathbf{A} & 0 \\ 0 & \mathbf{A} \end{bmatrix}$$

$$\Omega_j - \begin{bmatrix} \Omega & 0 \\ 0 & \Omega \end{bmatrix} \quad \Phi_j - \begin{bmatrix} \Phi & 0 \\ 0 & \Phi \end{bmatrix}$$

$$\Lambda_{\mathbf{R}} = \exp(-(\mathbf{R}_j + \Omega_j + \mathbf{K}_j + \mathbf{A}_j)T_{RF})$$

$$\Lambda = \exp(-(\mathbf{R}_j + \Omega_j + \mathbf{K}_j)(T_R - T_{RF}))$$

Experiment: Images were acquired from an adult male volunteer using a 3T GE MR750 scanner with a mcDESPOT protocol consisting of an SPGR image (8 flip angles), two SSFP images (0&180° phase-cycling, 8 flip angles) and an IR-SPGR image for B1 correction [4]. All scans used 800 μ s RF pulses. The images were processed to produce Myelin Water Fraction (MWF) images using both the derived finite pulse model and the previous instant pulse model. This work was approved by the King's College London Psychiatry Nursing and Midwifery ethics subcommittee.

Results: Example signal curves comparing finite pulses to instantaneous for a 2 pool model are shown in figure 1. These have been normalized to their mean value, as required for mcDESPOT processing [4]. Figure 2 shows an example sagittal slice through the MWF map processed with both models. When finite pulses are used for the analysis the calculated MWF is slightly but consistently higher by around 4% in white and grey matter.

Conclusion: Accounting for the finite length of the RF pulse can influence the reported MWF from mcDESPOT. At current pulse lengths the difference is small, but this discrepancy is expected to increase if longer pulse lengths are used to avoid magnetization transfer effects that are known to influence the bSSFP signal [5]. Further work with different pulse lengths is required to confirm this hypothesis.

Acknowledgements: We thank GE Healthcare for funding the scanning involved in this study.

References: (1) Bieri O, Scheffler K. SSFP signal with finite RF pulses. *Magnetic Resonance in Medicine*. 2009;62(5):1232–1241. (2) Jaynes ET. Matrix Treatment of Nuclear Induction. *Phys. Rev.* May 1955;98:1099–1105.0 (3) McConnell HM. Reaction Rates by Nuclear Magnetic Resonance. *Journal of Chemical Physics*. 1958;28(1). (4) Deoni SCL, Matthews L, Kolind SH. One component? Two components? Three? The effect of including a nonexchanging "free"water component in multicomponent driven equilibrium single pulse observation of T1 and T2. *Magnetic Resonance in Medicine*. 2012. (5) Gloor M, Scheffler K, Bieri O. Quantitative magnetization transfer imaging using balanced SSFP. *Magnetic Resonance in Medicine*. 2008;60(3):691–700.

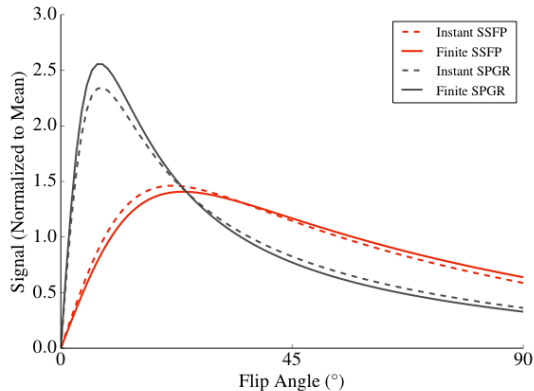


Figure 1 - Example SPGR and SSFP signals curves for a 2-pool model with instantaneous and finite RF pulses.

Figure 2 - Example MWF map processed with the finite pulse model (a), instant pulse model (b), and the difference between them (c). The finite pulse model reports consistently higher MWF values in white matter and grey matter.

